# Three-Dimensional Analysis of Morphologic Changes and Visual Outcomes in Neovascular Age-Related Macular Degeneration

Hyungwoo Lee, Aerin Jo, and Hyung Chan Kim

Department of Ophthalmology, Konkuk University Medical Center, Seoul, Republic of Korea

Correspondence: Hyung Chan Kim, Konkuk University Medical Center, 120-1 Neungdong-ro, Gwangjin-gu, Seoul 05030, Republic of Korea; eyekim@kuh.ac.kr.

Submitted: August 29, 2016
Accepted: January 8, 2017

Citation: Lee H, Jo A, Kim HC. Three-dimensional analysis of morphologic changes and visual outcomes in neovascular age-related macular degeneration. *Invest Ophthalmol Vis Sci*. 2017;58:1337–1345. DOI:10.1167/iovs.16-20637

**Purpose.** To investigate the association of three-dimensionally quantified lesions with best-corrected visual acuity (BCVA) in typical neovascular age-related macular degeneration (nAMD).

**Methods.** We retrospectively analyzed 65 eyes of 61 typical nAMD patients. Lesions at baseline and month 12 were manually delineated in optical coherence tomography. The volume of intraretinal fluid (IRF), subretinal fluid (SRF), subretinal hyperreflective material (SHRM), and pigment epithelial detachment (PED) were measured. In addition, the areas of external limiting membrane (ELM) and ellipsoid zone (EZ) were calculated.

**Results.** At baseline, poor baseline BCVA was associated with increased volume of IRF and SHRM and impaired area of ELM ($\beta = 0.34$, $P = 0.001$; $\beta = 0.46$, $P < 0.001$; and $\beta = -0.23$, $P = 0.03$, respectively). At month 12, poor BCVA was associated with increased volume of IRF, reduced intact ELM area, and decreased EZ area ($\beta = 0.24$, $P = 0.01$; $\beta = -0.30$, $P = 0.02$; and $\beta = -0.37$, $P = 0.004$, respectively). Baseline BCVA, volume of IRF, and intact area of ELM were significant predictors for BCVA at month 12 ($\beta = 0.29$, $P = 0.01$; $\beta = 0.30$, $P = 0.01$; and $\beta = -0.28$, $P = 0.01$). Changes of BCVA were associated with changes of SHRM volume, intact EZ area, and ELM area ($\beta = 0.35$, $P = 0.002$; $\beta = -0.28$, $P = 0.01$; and $\beta = -0.22$, $P = 0.048$, respectively). The predictive power of volumetric analysis was higher than that of qualitative analysis ($R^2 = 0.47$ vs. $R^2 = 0.37$). The volume of SRF and fibrovascular PED showed positive and negative effect on visual outcome each, but they were not strong enough to remain in multivariate model.

**Conclusions.** Best-corrected visual acuity could be explained by three-dimensional optical coherence tomography morphology to a fair degree. In addition, three-dimensional analysis could predict visual outcomes better than qualitative analysis.

Keywords: three-dimension, age-related macular degeneration, optical coherence tomography

Neovascular age-related macular degeneration (nAMD) is an important cause of blindness in elderly individuals in developed countries.[1] Spectral-domain optical coherence tomography (SD-OCT) is a useful imaging technique for diagnosing and treating patients with nAMD because it can visualize cross-sectional images of retinal microstructures with high resolution.[2]

Previous studies on visual prognostic factors using SD-OCT have shown that visual outcomes of nAMD could be explained by the presence of specific lesions, including intraretinal fluid (IRF), subretinal fluid (SRF), subretinal hyperreflective material (SHRM), pigment epithelial detachment (PED), and the integrity of ellipsoid zone (EZ) and external limiting membrane (ELM).[3–8] The majority of previous studies have investigated lesions at dichotomous status—the presence or absence at the fovea. However, retinal lesions exist as three-dimensional structures. Recent study has shown that the volumes of IRF, especially those located within 1000 μm of the foveal center, are mainly associated with visual outcomes of nAMD patients.[9] Therefore, we hypothesized that calculation of volumetric information of various pathomorphologic lesions (including SHRM and PED) and areal information of photoreceptor status in addition to the volumes of IRF and SRF could give us more accurate information of a patient's state.

In this study, we calculated the volumes of IRF, SRF, SHRM, PED, and the areas of intact EZ and ELM in nAMD patients. We determined the correlation of visual acuity at pretreatment and at month 12 with quantified lesions at each time point. We also examined the predictors for visual outcome. Finally, we compared the predictability of quantitative analysis on lesions with that of qualitative analysis.

## Methods

### Patients

We retrospectively reviewed medical records of typical nAMD patients treated in the Department of Ophthalmology at Konkuk University Medical Center between January 2010 and December 2015. At the initial visit, all patients underwent comprehensive ophthalmic examinations including measurement of best-corrected visual acuity (BCVA), intraocular pressure, slit-lamp biomicroscopy, color fundus photography, fluorescein angiography, indocyanine green angiography (ICGA), and SD-OCT using a Spectralis HRA+OCT (Heidelberg Engineering, Heidelberg, Germany). Eligible eyes had active choroidal neovascularization (CNV) secondary to AMD without

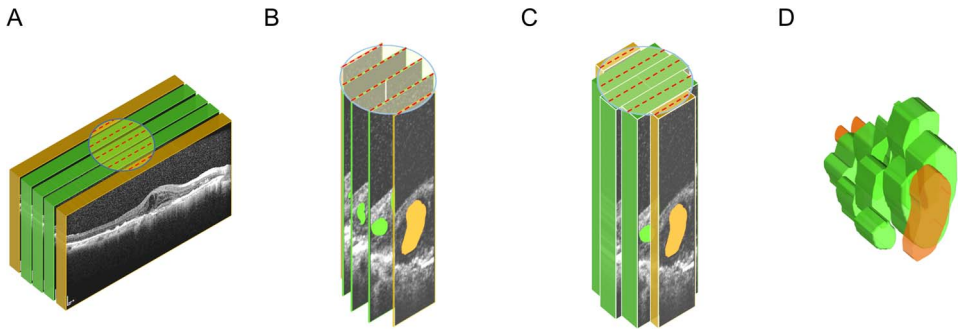


**Figure 1.** Construction of three-dimensional volume of morphologic factor from optical coherence tomography B-scans. (**A**) The thickness of five B-scans spanning macula was 250 μm. The blocks were cropped into a cylinder with a diameter of 1000 μm. (**B**) Five representative B-scans from the cylinder were selected. They were spaced 250 μm apart (*red dashed lines* on their top). Intraretinal fluid, SRF, SHRM, SPED, and FVPED were then manually segmented and their areas were calculated. (**C**) To obtain the volumes of delineated lesions, the areas were multiplied by their thicknesses (250 μm for central three blocks and 125 μm for both ends). (**D**) Five calculated volumes were summated to obtain the total volume of the lesion.

previous treatment. Exclusion criteria were: high myopia (>8 diopter), images obscured by media opacity, glaucoma, combined retinal diseases, significant cataract, and polypoidal choroidal vasculopathy (PCV). Polypoidal choroidal vasculopathy was diagnosed when polypoidal choroidal vascular dilations with branching vascular networks were observed on ICGA. We screened 224 patients who had diagnostic code of nAMD treated with at least 3 monthly ranibizumab injections. Among them, we excluded 83 patients with PCV and 15 patients with retinal angiomatous proliferation (RAP; type 3 neovascularization) by diagnostic codes and additional inspection on images. Among the remaining 126 typical nAMD patients, five patients with glaucoma and two patients with epiretinal membrane were also excluded. Fifty-eight patients were additionally excluded because of poor image qualities for delineation, missed follow-up, or omission of required medical records. This study followed the tenets of the Declaration of Helsinki. It was approved by the Institutional Review Board of Konkuk University Medical Center (KUH1100039).

Sixty-five eyes of 61 typical nAMD patients were treated with 3 monthly consecutive intravitreal injections of ranibizumab (0.5 mg/0.05 mL, Lucentis; Genentech, San Francisco, CA, USA). Additional injections were done on an as-needed basis if any of the following were observed: visual acuity reduction relative to the previous visit; recurrence or persistence of IRF, SRF, PED, and hemorrhage; increase of foveal thickness or increased angiographic leakage. When clinicians determined that ranibizumab injections could no longer improve visual acuity or lesion morphology, intravitreal bevacizumab injections were initiated on an as-needed basis (1.25 mg/0.05 mL, Avastin; Genentech). At each monthly visit, patients underwent exams including BCVA, fundus exam, color fundus photography, and SD-OCT.

## Image Analysis

Images at baseline and at months 12 were selected for analyses. Volume scans generated by SD-OCT covered an area of 9 mm × 6 mm with 25 scans spaced at 250 μm apart. Volumes of each lesion within 1000 μm of the foveal center was calculated with the following steps: (1) Whole B-scans were imported into ImageJ software version 1.50 (https://imagej.nih.gov/ij; provided in the public domain by the National Institutes of Health, Bethesda, MD, USA),[10] and each B-scan was duplicated into rectangular block with thickness of 250 μm (Fig. 1A). (2) The blocks were cropped into a cylinder with a diameter of 1000 μm. Five representative B-scans were selected from the cylinder, which was spaced 250 μm apart (Fig. 1B). The areas of IRF, SRF, SHRM, serous PED (SPED), and fibrovascular pigment epithelial detachment (FVPED) were manually segmented and calculated using open-source software (3D Slicer version 4.5; http://www.slicer.org; provided in the public domain by Harvard University, Cambridge, MA, USA).[11] For volume calculation, lesion areas were multiplied by their thickness (Fig. 1C, green central blocks: 250 μm, orange blocks: 125 μm). Total volume was calculated by summing the volumes of the five segments (Fig. 1D).

Intraretinal fluid was defined as round and hyporeflective spaces within the neurosensory retina. Subretinal fluid was identified as a hyporeflective space between the posterior surface of the neurosensory retina and the retinal pigment epithelium (RPE). Subretinal hyperreflective material was defined as hyperreflective material located external to neurosensory retina and internal to the RPE.[6] Serous PED was defined as elevations of RPE with internal hyporeflectivity. Fibrovascular pigment epithelial detachment was defined as elevations of RPE with heterogeneous internal reflectivity.[12] External limiting membrane was defined as a discrete hyperreflective band beneath the outer nuclear layer and above the EZ.[13] Ellipsoid zone was defined as the second hyperreflective band above the RPE. To measure the intact area of ELM and EZ within the cylinder, we used a similar method. Intact ELM and EZ line was lined in the five representative B-scans within the cylinder using ImageJ, and their lengths were measured from the 3D Slicer. The length was multiplied by the thickness of the scan to calculate the area as done for volume calculation.

## Statistical Analyses

Statistical analyses were performed using SPSS version 18.0 (SPSS, Chicago, IL, USA). Snellen visual acuity was converted to the logarithm of the minimal angle of resolution (logMAR) BCVA for statistical analyses. Statistical significance was considered when $P$ value was less than 0.05. Changes of factors after treatment were evaluated with paired $t$-test. Linear regression analyses were performed to find associated factors for visual acuity. Individual factors were analyzed by univariate regression analyses. They were entered for multivariate regression analysis in a stepwise manner if the $P$ value was less than 0.05. The relationship between baseline morphologic factors and intact photoreceptor area at month 12 was analyzed using Pearson correlation coefficient. Mann-Whitney $U$ test was performed to compare changes of BCVA of eyes with increased SHRM to other changes.

Investigative Ophthalmology & Visual Science

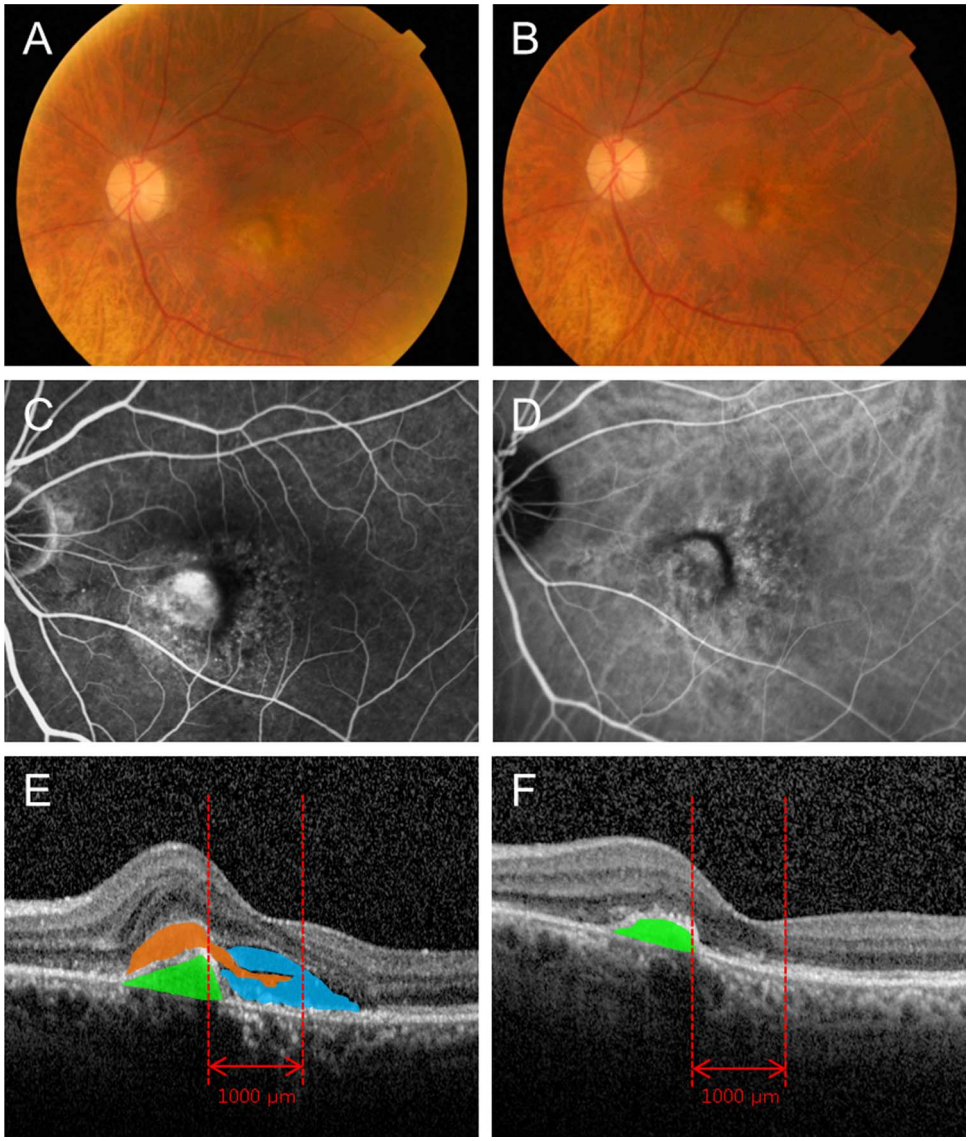


FIGURE 2. Changes of microstructures in a 74-year-old male patient. Initial visual acuity of 20/50 was improved to 20/30 after 12 months. (**A**) Fundus photography at baseline showing elevation of macula. (**B**) Fundus photography at month 12 showing resolved macular edema. (**C**) Diffuse leakage around macula at initial fluorescein angiography. (**D**) Initial ICGA showing no definite polypoidal lesion. (**E**) Horizontal B-scan of initial SD-OCT showing SRF (*blue color*), SHRM (*orange color*), and FVPED (*green color*). (**F**) Horizontal B-scan of SD-OCT at final visit showing resolution of SRF and SHRM. The height of PED is also decreased (*green color*).

## RESULTS

### Baseline Characteristics and Correlation With Visual Function

The study included 65 eyes of 61 patients (38 men and 23 women with average age of 74.1 ± 8.5 years). The mean follow-up period was 12.6 ± 0.9 months. The mean logMAR BCVA at baseline was 0.74 ± 0.50. Mean number of ranibizumab injection was 4.3 ± 1.5. Eight patients received additional 15 bevacizumab injections due to insufficient response to ranibizumab injections. Baseline morphologic factors IRF, SHRM, SRF, SPED, and FVPED were observed in 55.4%, 67.7%, 66.2%, 13.8%, and 81.5% of eyes, respectively. The mean volumes of these morphologic factors and the areas of intact photoreceptors were calculated within the 1000-μm diameter cylinder. Representative cases are shown in Figures 2 and 3. Specific results of visual acuity and pathomorphologic parameters are summarized in Table 1. To determine factors affecting baseline BCVA, regression analyses were performed. Univariate analysis showed that baseline BCVA was negatively associated with the volumes of IRF, SHRM, and FVPED ($\beta = 0.45$, $P < 0.001$; $\beta = 0.56$, $P < 0.001$; and $\beta = 0.25$, $P = 0.045$, respectively; Table 2). Intact areas of ELM and EZ at baseline were associated with good baseline BCVA ($\beta = -0.50$, $P < 0.001$ and $\beta = -0.30$, $P = 0.01$, respectively; Table 2). Multivariate regression analysis showed that poor baseline BCVA was associated with increased volumes of IRF, SHRM, and impaired ELM area ($\beta = 0.34$, $P = 0.001$; $\beta = 0.46$, $P < 0.001$; and $\beta = -0.23$, $P = 0.03$, respectively; Table 2).

### Prognostic Baseline Factors for Visual Outcome

We analyzed quantitative baseline factors associated with visual outcome. In univariate analysis, increased volumes of IRF and FVPED at baseline were associated with poor BCVA at month

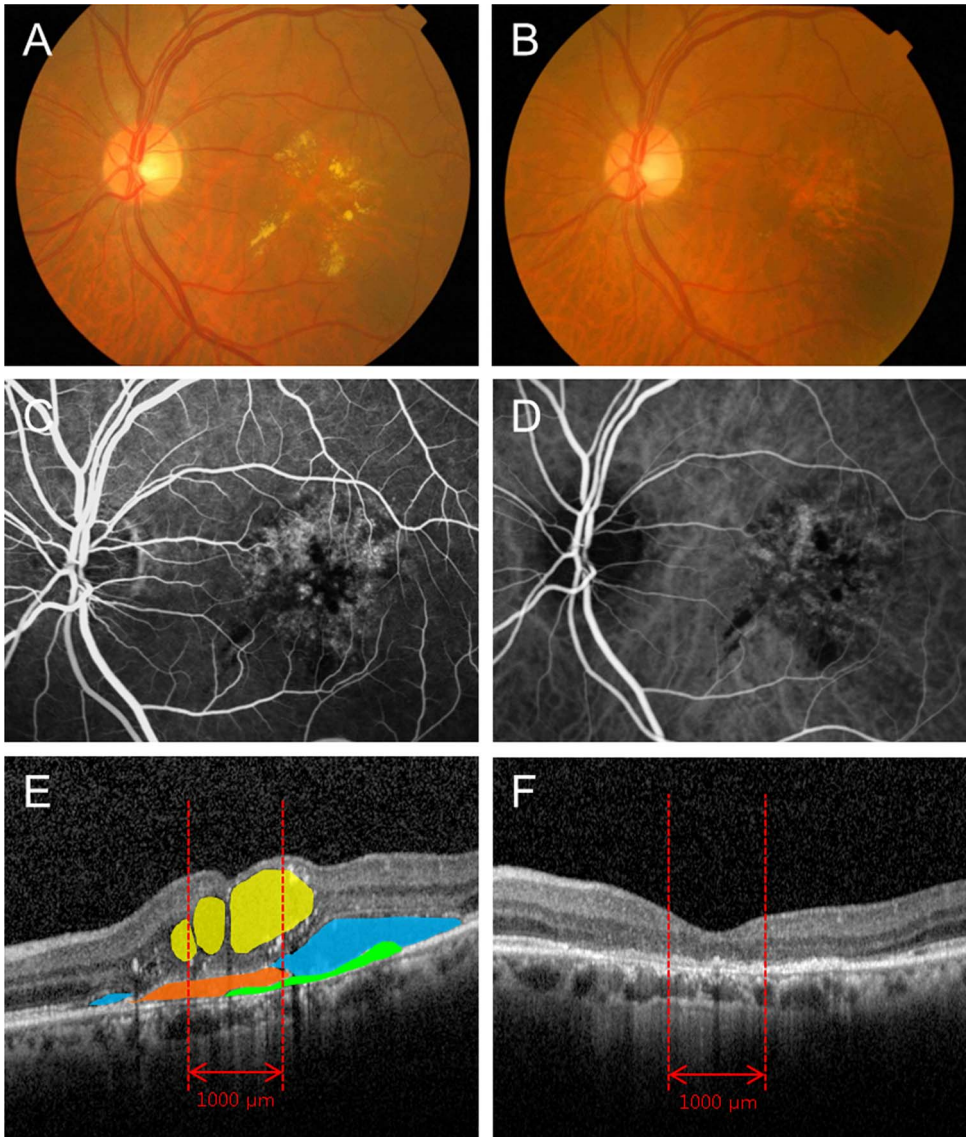


**Figure 3.** Changes of microstructures in a 78-year-old male patient. Initial visual acuity of 20/100 was stationary until month 12. (**A**) Fundus photography at baseline showing elevation of fovea and yellowish exudative materials at the parafoveal area. (**B**) Fundus photography at month 12 showing resolved macular edema and exudation. (**C**) Initial fluorescein angiography demonstrating CNV. (**D**) Initial ICGA showing no definite polypoidal lesion. (**E**) Horizontal B-scan of initial SD-OCT showing IRF (*yellow color*), SHRM (*orange color*), SRF (*blue color*), and thin fibrovascular PED (*green color*). (**F**) Horizontal B-scan of SD-OCT at month 12 visit showing resolution of IRF, SRF, and SHRM. Photoreceptor layers are damaged.

**Table 1.** Parameters at Baseline and Month 12

| Factors | Baseline | Month 12 | *P** |
|---|---|---|---|
| BCVA, logMAR | 0.74 ± 0.50 | 0.65 ± 0.53 | 0.34 |
| Volume, mm³ | | | |
| IRF | 0.03 ± 0.05 | 0.01 ± 0.03 | 0.002 |
| SRF | 0.04 ± 0.06 | 0.01 ± 0.05 | 0.02 |
| SHRM | 0.04 ± 0.06 | 0.02 ± 0.04 | 0.03 |
| SPED | 0.01 ± 0.04 | 0.001 ± 0.01 | 0.04 |
| FVPED | 0.04 ± 0.05 | 0.03 ± 0.04 | 0.01 |
| Area, mm² | | | |
| Intact ELM | 0.24 ± 0.24 | 0.36 ± 0.30 | 0.001 |
| Intact EZ | 0.12 ± 0.17 | 0.29 ± 0.29 | <0.001 |

* Paired *t*-test.

**Table 2.** Regression Analysis of Quantified Baseline Morphologic Factors for BCVA at Baseline

| | Univariate | | Multivariate | |
|---|---|---|---|---|
| Baseline Factors | Standardized Coefficient β | *P* | Standardized Coefficient β | *P* |
| Volume, mm³ | | | | |
| IRF | 0.45 | <0.001 | 0.34 | 0.001 |
| SRF | −0.17 | 0.19 | – | – |
| SHRM | 0.56 | <0.001 | 0.46 | <0.001 |
| SPED | −0.17 | 0.17 | – | – |
| FVPED | 0.25 | 0.045 | – | – |
| Area, mm² | | | | |
| Intact ELM | −0.50 | <0.001 | −0.23 | 0.03 |
| Intact EZ | −0.30 | 0.01 | – | – |

$R^2$ of multivariate regression model: 0.52.

**Table 3.** Regression Analysis of Baseline Quantitative/Qualitative Morphologic Factors for BCVA at Month 12

| | Quantitative Morphologic Factors | | | | | Qualitative Morphologic Factors | | | |
|---|---|---|---|---|---|---|---|---|---|
| | Univariate | | Multivariate | | | Univariate | | Multivariate | |
| Baseline Factors | Standardized Coefficient β | P | Standardized Coefficient β | P | Baseline Factors | Standardized Coefficient β | P | Standardized Coefficient β | P |
| BCVA, logMAR | 0.57 | <0.001 | 0.29 | 0.01 | BCVA, logMAR | 0.57 | <0.001 | 0.54 | <0.001 |
| Volume, mm³ | | | | | Presence | | | | |
| IRF | 0.53 | <0.001 | 0.30 | 0.01 | IRF | 0.31 | 0.01 | – | – |
| SRF | −0.30 | 0.01 | – | – | SRF | −0.34 | 0.01 | −0.27 | 0.01 |
| SHRM | 0.18 | 0.15 | – | – | SHRM | 0.04 | 0.78 | – | – |
| SPED | −0.21 | 0.09 | – | – | SPED | −0.19 | 0.14 | – | – |
| FVPED | 0.28 | 0.02 | – | – | FVPED | 0.28 | 0.03 | – | – |
| Area, mm² | | | | | Presence | | | | |
| Intact ELM | −0.53 | <0.001 | −0.28 | 0.01 | Intact ELM | −0.40 | 0.001 | – | – |
| Intact EZ | −0.30 | 0.01 | – | – | Intact EZ | −0.21 | 0.09 | – | – |

$R^2$ of multivariate regression model: 0.47 vs. 0.37.

12 ($\beta = 0.53$, $P < 0.001$ and $\beta = 0.28$, $P = 0.02$, respectively; Table 3). On the other hand, increased volume of SRF and intact areas of ELM and EZ at baseline were associated with good BCVA at month 12 ($\beta = -0.30$, $P = 0.01$; $\beta = -0.53$, $P < 0.001$; and $\beta = -0.30$, $P = 0.01$, respectively; Table 3). In addition, good baseline BCVA was also significantly associated with good posttreatment BCVA ($\beta = 0.57$, $P < 0.001$). In multivariate regression analysis, good baseline BCVA, small IRF volume, and intact ELM area at baseline were predictors for good BCVA at month 12 ($\beta = 0.29$, $P = 0.01$; $\beta = 0.30$, $P = 0.01$; and $\beta = -0.28$, $P = 0.01$, respectively; Table 3).

Next, we evaluated the prognostic power of qualitatively analyzed baseline factors, which were counted as "presence" when they spanned the fovea. In univariate regression analysis, good BCVA at month 12 was significantly associated with the absence of IRF or FVPED and the presence of SRF and intact ELM ($\beta = 0.31$, $P = 0.01$; $\beta = 0.28$, $P = 0.03$; $\beta = -0.34$, $P = 0.01$; and $\beta = -0.40$, $P = 0.001$, respectively; Table 3). In multivariate analysis, good BCVA at month 12 was associated with good baseline BCVA and the presence of SRF at baseline ($\beta = 0.54$, $P < 0.001$ and $\beta = -0.27$, $P = 0.01$; respectively; Table 3). The $R^2$ of the multivariate regression model implying the explanatory power for BCVA was 0.37. The $R^2$ of the former model from quantified baseline factors was 0.47.

**Table 4.** Regression Analysis of Quantitative Morphologic Factors at Month 12 for BCVA at Month 12

| | Univariate | | Multivariate | |
|---|---|---|---|---|
| Factors at Month 12 | Standardized Coefficient β | P | Standardized Coefficient β | P |
| Volume, mm³ | | | | |
| IRF | 0.42 | 0.001 | 0.24 | 0.01 |
| SRF | 0.03 | 0.82 | – | – |
| SHRM | 0.46 | <0.001 | – | – |
| SPED | −0.13 | 0.29 | – | – |
| FVPED | 0.24 | 0.06 | – | – |
| Area, mm² | | | | |
| Intact ELM | −0.66 | <0.001 | −0.30 | 0.02 |
| Intact EZ | −0.65 | <0.001 | −0.37 | 0.004 |

$R^2$ of multivariate regression model: 0.55.

## Morphologic Factors and Visual Acuity at Month 12

At month 12, good BCVA was associated with small volumes of both IRF and SHRM and with large area of intact ELM and EZ in univariate regression analysis ($\beta = 0.42$, $P = 0.001$; $\beta = 0.46$, $P < 0.001$; $\beta = -0.66$, $P < 0.001$; and $\beta = -0.65$, $P < 0.001$, respectively; Table 4). In multivariate regression analysis, good BCVA at month 12 was significantly associated with small IRF volume, intact ELM area, and intact EZ area ($\beta = 0.24$, $P = 0.01$; $\beta = -0.30$, $P = 0.02$; and $\beta = -0.37$, $P = 0.004$, respectively; Table 4).

## Morphologic Factors Associated With Visual Acuity Change

Sixteen eyes (24.6%) lost more than 0.3 logMAR BCVA at month 12. The association between quantified baseline factors and BCVA change was investigated. In univariate regression analysis, BCVA was significantly improved when baseline BCVA was poor and SHRM volume was increased ($\beta = -0.42$, $P = 0.001$ and $\beta = -0.38$, $P = 0.002$, respectively; Table 5). In multivariate regression analysis, only poor baseline BCVA was a prognostic factor for the improvement of BCVA ($\beta = -0.42$, $P = 0.001$; Table 5).

Next, we analyzed the correlation between BCVA change and quantitative change of morphologic factors. As shown in Table 1, all volumes of IRF, SRF, SHRM, SPED, and FVPED were significantly decreased while the intact areas of both ELM and EZ were increased after 12 months. Among them, the improvement of BCVA was correlated with the reduction of SHRM volume and the increase of intact areas of ELM and EZ in univariate regression analysis ($\beta = 0.51$, $P < 0.001$; $\beta = -0.43$, $P < 0.001$; and $\beta = -0.46$, $P < 0.001$, respectively; Table 5). The volume of SHRM and the intact area of EZ remained significant in the multivariate regression model while the change of ELM area was marginally significant for BCVA change ($\beta = 0.35$, $P = 0.002$; $\beta = -0.28$, $P = 0.01$; and $\beta = -0.22$, $P = 0.048$, respectively; Table 5). There were 28 eyes (43.1%) with SHRM at month 12 compared to 43 eyes (67.7%) at baseline. Among those 28 eyes, SHRM volume was increased in 14 eyes (50.0%) compared to that at baseline. The BCVA improvement in eyes

**Table 5.** Factors Associated With the Change of BCVA

| | Baseline Factors | | | | Changes of Factors | | | |
|---|---|---|---|---|---|---|---|---|
| | Univariate | | Multivariate | | Univariate | | Multivariate | |
| Factors | Standardized Coefficient β | *P* | Standardized Coefficient β | *P* | Standardized Coefficient β | *P* | Standardized Coefficient β | *P* |
| BCVA, logMAR | −0.42 | 0.001 | −0.42 | 0.001 | – | – | – | – |
| Volume, mm³ | | | | | | | | |
| IRF | 0.13 | 0.32 | – | – | 0.06 | 0.61 | – | – |
| SRF | −0.16 | 0.22 | – | – | 0.20 | 0.10 | – | – |
| SHRM | −0.38 | 0.002 | – | – | 0.51 | <0.001 | 0.35 | 0.002 |
| SPED | −0.04 | 0.75 | – | – | 0.04 | 0.77 | – | – |
| FVPED | 0.05 | 0.72 | – | – | 0.16 | 0.21 | – | – |
| Area, mm² | | | | | | | | |
| Intact ELM | −0.07 | 0.58 | – | – | −0.43 | <0.001 | −0.22 | 0.048 |
| Intact EZ | −0.03 | 0.83 | – | – | −0.46 | <0.001 | −0.28 | 0.01 |

$R^2$ of multivariate regression model: 0.17 vs. 0.40.

with increased SHRM was significantly ($P = 0.01$) poorer than that in others.

## Correlation Between Photoreceptor Integrity and Morphologic Factors

The intact ELM area at month 12 had a negative correlation with baseline IRF volume but a positive correlation with baseline SRF volume and baseline intact ELM or EZ area ($r = -0.56$, $P < 0.001$; $r = 0.36$, $P = 0.003$; $r = 0.52$, $P < 0.001$; and $r = 0.35$, $P = 0.005$, respectively; Table 6). The intact EZ area at month 12 was correlated negatively with baseline IRF volume but positively with baseline intact ELM or EZ area ($r = -0.47$, $P < 0.001$; $r = 0.44$, $P < 0.001$; and $r = 0.40$, $P = 0.001$, respectively; Table 6). The increases of intact ELM and EZ area were both correlated with the reduction of SHRM volume ($r = -0.33$, $P = 0.007$ and $r = -0.29$, $P = 0.019$, respectively).

## Discussion

In the present study, we investigated the associations between morphologic factors and visual outcome in typical nAMD using quantitative analysis of SD-OCT. Previous studies have investigated the associations between structures in SD-OCT and visual outcome in nAMD patients and found that the presence of IRF, SRF, SHRM, or PED and disruption of ELM or EZ are related to visual outcomes.[3,5–8] Majority of them have described morphologic lesions as presence or absence with one-dimensional (i.e., height, width) or two-dimensional traits (i.e., area). To obtain more realistic information, recent studies have tried to get three-dimensional information from volume scan of SD-OCT.[9,14–17] These pioneering studies have reconstructed morphologic lesions based on SD-OCT and found that three-dimensional characteristics could successfully explain the visual outcome of nAMD patients. Because those studies only focused on several selected factors, we quantified various pathomorphologic factors and investigated their effects on BCVA at baseline and month 12 as well as BCVA change.

**Table 6.** Correlation Between Intact Photoreceptor Area at Month 12 and Baseline Morphologic Factors

| | Intact ELM Area at Month 12 | | Intact EZ Area at Month 12 | |
|---|---|---|---|---|
| Baseline Factors | *r** | *P* | *r** | *P* |
| Volume, mm³ | | | | |
| IRF | −0.56 | <0.001 | −0.47 | <0.001 |
| SRF | 0.36 | 0.003 | 0.17 | 0.17 |
| SHRM | −0.06 | 0.65 | −0.06 | 0.65 |
| SPED | −0.03 | 0.81 | −0.01 | 0.96 |
| FVPED | −0.17 | 0.20 | −0.14 | 0.27 |
| Area, mm² | | | | |
| Intact ELM | 0.52 | <0.001 | 0.44 | <0.001 |
| Intact EZ | 0.35 | 0.005 | 0.40 | 0.001 |

* $r$ = Pearson's correlation coefficient.

In our study, increased volume of IRF and disruption of intact ELM area at baseline were associated with poor BCVA at baseline, consistent with previous studies using quantitative approaches.[9,16] Furthermore, baseline IRF volume and baseline intact area of ELM were predictive of poor visual outcome at month 12, consistent with previous studies using nonquantitative approaches.[3,4,8] However, for prediction of visual outcome at month 12, previous quantitative studies on IRF have reported conflicting results. Waldstein et al.[9] have found significant correlation between BCVA at month 12 and baseline optimized area indicator of IRF, which accentuated the central areas with IRF height up to 20 μm. On the other hand, Roberts et al.[16] have found no correlation between the area of IRF and posttreatment BCVA. Our result suggested that the volume of IRF within 1000-μm diameter of cylinder was a significant prognostic factor for BCVA at month 12.

The persistent negative effect of baseline IRF on BCVA at month 12 might be due to impaired signal transduction. Because bipolar cells connect the signal from photoreceptors to ganglion cell, their excessive mechanical stretching by IRF could result in dysfunction of bipolar cells as suggested in a previous study using microscopic data.[18] There was a negative correlation between the volume of baseline IRF and the intact photoreceptor area at month 12 in this study. Although the mechanism of IRF formation remains unclear, inflammatory environment could impair the function of RPE, which removes water outside the retina, eventually forming IRF.[19] On the other hand, Müller cells can control homeostasis of water and ionic concentration in the interstitial area and manage the products of metabolism of associated neural cells.[20] Previous study has shown that Müller cells are activated in AMD.[21] They seem to be harmful under pathologic conditions by secreting proangiogenic factors such as VEGF.[22,23] Although the role of activated

Müller cells in nAMD remains unclear, their loss of function to sustain water balance might induce the formation of IRF. This inflammatory environment could also simultaneously damage the integrity of photoreceptor. Therefore, the predictive power of IRF volume for poor visual outcome could be explained by abnormal function of RPE and Müller cells accompanied by photoreceptor impairment.

In this study, ELM area was another predictor associated with visual outcome at month 12, consistent with results of a previous study.[16] External limiting membrane is thought to be essential for photoreceptor function. Disruption of ELM significantly affects visual impairment.[24,25] In the multivariate regression model, intact ELM area and IRF volume at baseline were selected as significant quantitative factors that could creditably explain visual prognosis. Therefore, ELM area and IRF volume could be used as good prognostic factors for visual acuity at month 12. Among all baseline factors, baseline BCVA was the most powerful predictor of BCVA at month 12. Although direct comparison of our results with other quantitative studies is inappropriate due to different conditions, the construction of a prognostic model from various quantitative morphologic factors is one strength of this present study.

With regard to morphologic factors at month 12, IRF volume and intact ELM area were still significant factors explaining BCVA at month 12. In addition, reduction of intact EZ area was another significant factor associated with poor BCVA, consistent with results of previous qualitative studies.[5,25] On the other hand, change of IRF volume was not associated with change of BCVA. These results might imply that impaired visual function is only partly reversible by anti-VEGF treatment when IRF volume persists significantly.

Next, we investigated the associated factors for change of visual acuity. Patients with poor baseline BCVA had more chance to improve visual acuity than those with good baseline BCVA, consistent with results of previous studies.[26,27] Interestingly, SHRM volume was the only volumetric factor associated with BCVA change. Although increased SHRM volume was correlated with poor BCVA at baseline, thick SHRM at baseline was associated with statistically significant BCVA improvement after 12 months. The amount of SHRM volume reduction was also associated with BCVA increment, consistent with results of previous qualitative and quantitative studies.[6,17] This phenomenon could be explained by the recovery of photoreceptor because the reduction of SHRM volume was associated with the increment of intact ELM and EZ area. Subretinal hyperreflective material has various elements, including fluid, blood, fibrovascular tissue, and CNV in the subretinal area.[6] These materials could damage the overlying ELM and EZ and impair the visual acuity at baseline. However, this effect is likely reversible in contrast to IRF-induced damage. Therefore, new approaches to reduce SHRM might help patients gain visual acuity. For example, antifibrotic agents might act as an adjunctive therapy to reduce fibrous components in SHRM (Whitlock A, et al. *IOVS* 2014;55:ARVO E-Abstract 1203).

The volume of SRF seemed to have positive effect on visual outcome. Baseline SRF volume was associated with good final BCVA in univariate regression analysis, although such relationship was not significant in multivariate regression analysis. In qualitative analysis of our study, the presence of SRF spanning fovea was a strong predictor of good visual prognosis. Recent studies using qualitative and quantitative methods have also found a weak positive effect of SRF on visual outcome.[5,9,27] Taken together, at least SRF might be harmless to visual prognosis. It might have beneficial effect.[5,9,27] Subretinal fluid could serve as a buffer to protect photoreceptor from direct appositional damage caused by active inflammatory CNV lesion. Further study is needed to clarify the role of SRF.

The role of PEDs on visual outcome remains ambiguous. Baseline volume of FVPED, not of SPED, was associated with poor BCVA both at baseline and month 12 in the univariate regression analysis of this study, but not in the multivariate regression model. Changes of BCVA showed no correlation with volumetric changes of either type of PED. Similarly, a previous study has reported that the presence of FVPED at baseline is associated with poor visual outcome while the resolution of FVPED is not correlated with visual gain.[28] From these results, FVPED might be associated with irreversible damage on visual function, like IRF volume. However, the route of negative effect remains unclear. Intact photoreceptor area at month 12 was not correlated with the volume of PED at baseline. All results about PEDs in our study were not strong enough to be remained in multivariate regression model. Therefore, the effect of PEDs on visual outcome needs to be confirmed by further studies.

Finally, we investigated whether the prognostic power using volumetric quantification of factors was superior over qualitative classification. Although dichotomous classification could easily provide interpretable information on the state, we hypothesized that this approach could miss detailed information of three-dimensional structures and lead to weak predictive power for visual outcome. Regression analysis using baseline qualitative classification showed that the presence of baseline IRF, SRF, and the disruption of photoreceptor could predict visual outcome as in volumetric analysis. However, $R^2$ of the regression model using qualitative analysis was 0.37, which was lower than 0.47 from volumetric quantification. $R^2$ indicates how much the regression model can explain visual prognosis. From this result, volumetric analysis of morphologic factors could be a good alternative of qualitative analysis to predict visual outcome.

On the other hand, visual prognosis showed no statistically significant improvement and the number of injections of our cohort was relatively lower than that in other reports.[29] Because the National Health Insurance system of South Korea covers a limited number of ranibizumab injections, the number of injections in our study might have been lower than that in other countries as shown in another study in South Korea.[30] In addition, the exclusion of PCV might have reduced the number of injections because there are cases that require frequent injections.[31] In addition, there were still 28 eyes (43.1%) with SHRM at month 12, and half of them had increased SHRM volumes with significantly lower increases of BCVA. This substantial proportion of increased SHRM after treatment might have hindered the improvement of BCVA.

This study has several limitations. First, only volumetric information of lesions within a 1000-μm diameter of cylinder was obtained because the previous study of Waldstein et al.[9] has shown that lesion within 1000 μm diameter was mainly associated with visual outcome. The spatial weighting function depending on the location, which was used in their study,[9] might be considered in a further study because the density of photoreceptors could be reduced as the location is getting away from the foveola. Developing customized software for SD-OCT images could solve these problems. Although we could not calculate sophisticated functions, our study has implications for implementing volume and area calculation within cylinder space with noncommercial open source programs ImageJ and 3D Slicer. Second, the wide spacing of B-scans (250 μm apart) in our study could not fully reflect the real morphology of lesions. Denser B-scans might allow us to get more precise information and lead to better predictions for visual outcome. Third, the study population was limited to typical nAMD patients. Because of different characteristics and

prognosis of PCV and RAP, we did not include those patients to avoid confounding statistical results from mixed disease entities.[32] To understand the nAMD comprehensively, further study should be done by including PCV and RAP patients and comparing the effects of three-dimensional aspects on prognosis between the two types of nAMD. Fourth, volumetric analysis is not readily applicable to clinical setting because manual delineation is a time-consuming and elaborative process. The ImageJ and 3D Slicer software programs we used were convenient to reconstruct the volume. However, their automatic demarcation ability was not enough to find the exact edge of structures, leading to manual correction. Recent studies have started to develop software based on machine learning algorithms with successful results in delineating fluid edge.[33,34] Further studies on these algorithms will allow us to obtain volumetric information more quickly and accurately in clinical settings. Finally, the retrospective nature of this study and small number of patients are also the limitations of this study. Further prospective and randomized clinical studies will be required.

In conclusion, volumetric analysis on SD-OCT is a useful approach to explain visual status. It can be used to predict visual outcome of typical nAMD patients.

## Acknowledgments

Disclosure: **H. Lee**, None; **A. Jo**, None; **H.C. Kim**, None

## References

1. Seddon JM, Chen CA. The epidemiology of age-related macular degeneration. *Int Ophthalmol Clin*. 2004;44:17–39.
2. Keane PA, Liakopoulos S, Jivrajka RV, et al. Evaluation of optical coherence tomography retinal thickness parameters for use in clinical trials for neovascular age-related macular degeneration. *Invest Ophthalmol Vis Sci*. 2009;50:3378–3385.
3. Ritter M, Simader C, Bolz M, et al. Intraretinal cysts are the most relevant prognostic biomarker in neovascular age-related macular degeneration independent of the therapeutic strategy. *Br J Ophthalmol*. 2014;98:1629–1635.
4. Simader C, Ritter M, Bolz M, et al. Morphologic parameters relevant for visual outcome during anti-angiogenic therapy of neovascular age-related macular degeneration. *Ophthalmology*. 2014;121:1237–1245.
5. Jaffe GJ, Martin DF, Toth CA, et al. Macular morphology and visual acuity in the comparison of age-related macular degeneration treatments trials. *Ophthalmology*. 2013;120:1860–1870.
6. Willoughby AS, Ying GS, Toth CA, et al. Subretinal hyperreflective material in the comparison of age-related macular degeneration treatments trials. *Ophthalmology*. 2015;122:1846–1853.
7. Schmidt-Erfurth U, Waldstein SM, Deak GG, Kundi M, Simader C. Pigment epithelial detachment followed by retinal cystoid degeneration leads to vision loss in treatment of neovascular age-related macular degeneration. *Ophthalmology*. 2015;122:822–832.
8. Mathew R, Richardson M, Sivaprasad S. Predictive value of spectral-domain optical coherence tomography features in assessment of visual prognosis in eyes with neovascular age-related macular degeneration treated with ranibizumab. *Am J Ophthalmol*. 2013;155:720–726.
9. Waldstein SM, Philip AM, Leitner R, et al. Correlation of 3-dimensionally quantified intraretinal and subretinal fluid with visual acuity in neovascular age-related macular degeneration. *JAMA Ophthalmol*. 2016;134:182–190.
10. Rasband WS. ImageJ (version 1.50). Bethesda, Maryland: National Institutes of Health. Available at: http://imagej.nih.gov/ij/. Accessed April 1, 2016.
11. Fedorov A, Beichel R, Kalpathy-Cramer J, et al. 3D Slicer as an image computing platform for the Quantitative Imaging Network. *Magn Reson Imaging*. 2012;30:1323–1341.
12. Coscas F, Coscas G, Souied E, Tick S, Soubrane G. Optical coherence tomography identification of occult choroidal neovascularization in age-related macular degeneration. *Am J Ophthalmol*. 2007;144:592–599.
13. Staurenghi G, Sadda S, Chakravarthy U, Spaide RF. Proposed lexicon for anatomic landmarks in normal posterior segment spectral-domain optical coherence tomography: the IN*OCT consensus. *Ophthalmology*. 2014;121:1572–1578.
14. Golbaz I, Ahlers C, Stock G, et al. Quantification of the therapeutic response of intraretinal, subretinal, and subpigment epithelial compartments in exudative AMD during anti-VEGF therapy. *Invest Ophthalmol Vis Sci*. 2011;52:1599–1605.
15. Ristau T, Hillebrand S, Smailhodzic D, et al. Prognostic factors for long term visual acuity outcome after ranibizumab therapy in patients with neovascular age-related macular degeneration. *J Clin Exp Ophthalmol*. 2013;4:264.
16. Roberts P, Mittermueller TJ, Montuoro A, et al. A quantitative approach to identify morphological features relevant for visual function in ranibizumab therapy of neovascular AMD. *Invest Ophthalmol Vis Sci*. 2014;55:6623–6630.
17. Charafeddin W, Nittala MG, Oregon A, Sadda SR. Relationship between subretinal hyperreflective material reflectivity and volume in patients with neovascular age-related macular degeneration following anti-vascular endothelial growth factor treatment. *Ophthalmic Surg Lasers Imaging*. 2015;46:523–530.
18. Pelosini L, Hull CC, Boyce JF, McHugh D, Stanford MR, Marshall J. Optical coherence tomography may be used to predict visual acuity in patients with macular edema. *Invest Ophthalmol Vis Sci*. 2011;52:2741–2748.
19. Dahrouj M, Alsarraf O, McMillin JC, Liu Y, Crosson CE, Ablonczy Z. Vascular endothelial growth factor modulates the function of the retinal pigment epithelium in vivo. *Invest Ophthalmol Vis Sci*. 2014;55:2269–2275.
20. Spaide RF. Retinal vascular cystoid macular edema: review and new theory. *Retina*. 2016;36:1823–1842.
21. Guidry C, Medeiros NE, Curcio CA. Phenotypic variation of retinal pigment epithelium in age-related macular degeneration. *Invest Ophthalmol Vis Sci*. 2002;43:267–273.
22. Amin RH, Frank RN, Kennedy A, Eliott D, Puklin JE, Abrams GW. Vascular endothelial growth factor is present in glial cells of the retina and optic nerve of human subjects with nonproliferative diabetic retinopathy. *Invest Ophthalmol Vis Sci*. 1997;38:36–47.
23. Eichler W, Yafai Y, Wiedemann P, Reichenbach A. Angiogenesis-related factors derived from retinal glial (Muller) cells in hypoxia. *Neuroreport*. 2004;15:1633–1637.
24. Oishi A, Hata M, Shimozono M, Mandai M, Nishida A, Kurimoto Y. The significance of external limiting membrane status for visual acuity in age-related macular degeneration. *Am J Ophthalmol*. 2010;150:27–32.
25. Shin HJ, Chung H, Kim HC. Association between foveal microstructure and visual outcome in age-related macular degeneration. *Retina*. 2011;31:1627–1636.
26. Ying GS, Huang J, Maguire MG, et al. Baseline predictors for one-year visual outcomes with ranibizumab or bevacizumab for neovascular age-related macular degeneration. *Ophthalmology*. 2013;120:122–129.
27. Waldstein SM, Simader C, Staurenghi G, et al. Morphology and visual acuity in aflibercept and ranibizumab therapy for

neovascular age-related macular degeneration in the VIEW Trials. *Ophthalmology*. 2016;123:1521–1529.

28. Inoue M, Arakawa A, Yamane S, Kadonosono K. Variable response of vascularized pigment epithelial detachments to ranibizumab based on lesion subtypes, including polypoidal choroidal vasculopathy. *Retina*. 2013;33:990–997.
29. Ferreira A, Sagkriotis A, Olson M, Lu J, Makin C, Milnes F. Treatment frequency and dosing interval of ranibizumab and aflibercept for neovascular age-related macular degeneration in routine clinical practice in the USA. *PLoS One*. 2015;10: e0133968.
30. Kim JH, Lee DW, Chang YS, Kim JW, Kim CG. Twelve-month outcomes of treatment using ranibizumab or aflibercept for neovascular age-related macular degeneration: a comparative study. *Graefes Arch Clin Exp Ophthalmol*. 2016;254:2101–2109.
31. Lee JH, Lee WK. Anti-vascular endothelial growth factor monotherapy for polypoidal choroidal vasculopathy with polyps resembling grape clusters. *Graefes Arch Clin Exp Ophthalmol*. 2016;254:645–651.
32. Wong CW, Yanagi Y, Lee WK, et al. Age-related macular degeneration and polypoidal choroidal vasculopathy in Asians. *Prog Retin Eye Res*. 2016;53:107–139.
33. Chiu SJ, Allingham MJ, Mettu PS, Cousins SW, Izatt JA, Farsiu S. Kernel regression based segmentation of optical coherence tomography images with diabetic macular edema. *Biomed Opt Express*. 2015;6:1172–1194.
34. Chiu SJ, Izatt JA, O'Connell RV, Winter KP, Toth CA, Farsiu S. Validated automatic segmentation of AMD pathology including drusen and geographic atrophy in SD-OCT images. *Invest Ophthalmol Vis Sci*. 2012;53:53–61.

Investigative Ophthalmology & Visual Science